Report

Fluorescent Tools to Analyze Peroxisome–Endoplasmic Reticulum Interactions in Mammalian Cells

Contact
Volume 2: 1–14
© The Author(s) 2019
DOI: 10.1177/2515256419848641
journals.sagepub.com/home/ctc
SAGE

Alexa Bishop[1, 2, *], Maki Kamoshita[1, *], Josiah B. Passmore[1], Christian Hacker[1], Tina A. Schrader[1], Hans R. Waterham[3], Joseph L. Costello[1, #] and Michael Schrader[1, #]

Abstract

Peroxisomes (POs) and the endoplasmic reticulum (ER) cooperate extensively in lipid-related metabolic pathways, and the ER also provides phospholipids to enable the peroxisomal membrane to expand prior to division. Recently, we identified peroxisomal proteins, ACBD5 and ACBD4, and the ER protein vesicle-associated membrane protein-associated protein-B (VAPB) as tethering components, which physically interact to foster PO–ER associations at membrane contact sites. Overexpression or loss of these tether proteins alters the extent of PO–ER interactions, impacting on lipid exchange between these two compartments. To facilitate further studies into PO–ER associations at the level of membrane contact sites, their role, composition, and regulation, we have developed two fluorescence-based systems to monitor PO–ER interactions. We modified a proximity ligation assay and a split-fluorescence reporter system using split superfolder green fluorescent protein. Using the proximity ligation assay, we were able to measure the changes in PO–ER interactions while the split-fluorescence reporter was more limited and only allowed us to label PO–ER contacts. We show that both techniques can be useful additions to the toolkit of methods to study PO–ER associations and explore the relative merits of each.

Keywords

peroxisomes, ER, ACBD5, VAPB, membrane contact sites

Introduction

In the complex, condensed environment of the eukaryotic cell, intricate communication and collaboration between different organelles ensure that biological processes are precisely coordinated. Despite each organelle performing its own specific role, interaction with other organelles is essential and establishing such interactions involves close, physical contacts, generally maintained via specific protein complexes, which facilitate the bringing together of organelle membranes at membrane contact sites (Cohen, Valm, & Lippincott-Schwartz, 2018). Recent work suggests that most, if not all, organelles communicate in this way and numerous protein complexes contributing to organelle interaction and tethering have been identified, in particular those involved in mediating associations between the endoplasmic reticulum (ER) and the mitochondria (Eisenberg-Bord, Shai, Schuldiner, & Bohnert, 2016; Gatta & Levine, 2017). ER–mitochondria interactions allow a multitude of exchange events including Ca^{2+} and lipid transport and also regulate mitochondrial division (Friedman et al., 2011; Lewis, Uchiyama, & Nunnari, 2016;

[1]Biosciences, University of Exeter, UK
[2]Centre for Vascular Biology, Institute of Molecular and Clinical Sciences, St George's, University of London, UK
[3]Laboratory Genetic Metabolic Diseases, Department of Clinical Chemistry, Academic Medical Center, Amsterdam, the Netherlands

Received December 20, 2018. Revised April 12, 2019. Accepted April 13, 2019.

*These authors share equal first author contribution.
#These authors share equal senior author contribution.

Corresponding Author:
Joseph L. Costello, Biosciences, University of Exeter, Exeter EX4 4QD, UK.
Email: J.Costello@exeter.ac.uk
Michael Schrader, Biosciences, University of Exeter, Exeter EX4 4QD, UK.
Email: m.schrader@exeter.ac.uk

Rizzuto et al., 1998; Vance, 1990). Quantification of organelle interaction has often utilized electron microscopy (EM) to assess both the number and the extent of membrane proximity events in the <30 nm range as the gold standard for this assay (Helle et al., 2013). However, EM studies are often not compatible with screening and high-throughput approaches and require fixation so cannot be used to assess interaction dynamics. We aimed to establish straightforward techniques to give a rapid readout of peroxisome (PO)–ER contacts, without relying on specialist facilities, which could complement EM studies and allow a higher throughput analysis of PO–ER contacts. Recently, several fluorescence-based techniques have been used in both yeast and mammalian cells to assess organelle–ER associations, including proximity ligation assays (PLAs; Alpy et al., 2013; Stoica et al., 2016; Tubbs & Rieusset, 2016; Tubbs et al., 2014) and split-fluorescence technology (Alford, Ding, Simmen, & Campbell, 2012; Cieri et al., 2018; Kakimoto et al., 2018; Yang, Zhao, Xu, Shang, & Tong, 2018). The PLA (see Figure 1(a)) involves antibodies targeted to proteins on apposing membranes of different organelles in close proximity. Oligonucleotide proximity probes fused to secondary antibodies can then be ligated, allowing signal amplification and subsequent binding of fluorescently labeled probes. Split-fluorescence assays, such as split superfolder green fluorescent protein (spGFP), rely on targeting nonfluorescent portions of a fluorescent protein to different organelle membranes. Individually, the two portions do not fluoresce but reconstitution of the fluorescent signal occurs when the split portions rejoin, indicating close proximity of the two organelles. These assays have both complemented and extended EM studies, allowing greater characterization of dynamic ER–mitochondria interactions.

POs are another organelle which interacts extensively with the ER. POs and the ER cooperate in a number of lipid-related processes (e.g., the synthesis of etherphospholipids and polyunsaturated fatty acids such as docosahexaenoic acid) and are often found in close association in cells (Schrader et al., 2015; Schrader, Kamoshita, & Islinger, 2019). These interactions were initially observed in ultrastructural studies in different cell types and display close, intimate interactions, with ER cisternae often observed wrapping around spherical peroxisomal structures (Novikoff & Novikoff, 1972; Zaar, Völkl, & Fahimi, 1987). Recently, we and others showed that PO–ER associations can be mediated by direct interaction at the level of membrane contact sites, where the two organelle membranes are brought into close proximity in the 15 nm range, mediated by interaction between the peroxisomal membrane proteins ACBD5 and ACBD4 and the ER protein vesicle-associated membrane protein-associated protein-B (VAPB; Costello, Castro, Hacker, et al., 2017; Costello, Castro, Schrader, Islinger, & Schrader, 2017; Hua et al., 2017). We previously employed EM to quantify the association between POs and the ER (Costello, Castro, Hacker, et al., 2017). Here, we developed a PLA and split-fluorescence assay to allow the analysis of PO–ER associations in mammalian cells. We explore the benefits and drawbacks of these techniques and confirm that although the PLA was not able to detect all PO–ER interactions, it could be used to measure changes in the association between the organelles. The split-fluorescence reporter appeared to show evidence of irreversibility, but it did allow us to label prominent interaction sites between POs and the ER, helping explore our proposed model for this interaction.

Results and Discussion

PLAs Can Be Used as a Measure of PO–ER Associations

The original PLA allowed individual pairs of interacting proteins to be identified in fixed cells using an antibody-based approach (Söderberg et al., 2006). This relies on the binding of primary antibodies to the two proteins of interest followed by the addition of secondary antibodies fused to oligonucleotide proximity probes. If the two proteins of interest are within 40 nm of each other, the proximity probes can then ligate with connector oligonucleotides to form a circular DNA strand which acts as a template, allowing signal amplification and subsequent binding of fluorescently labeled probes (see Figure 1(a)). The end result is the formation of discrete fluorescent PLA signals where the two proteins interact. Recent studies have adapted the original PLA for measuring protein–protein interactions to instead measure the extent of organelle interactions by using primary antibodies against proteins found on apposing membranes at the ER–mitochondria interface (Tubbs & Rieusset, 2016). For example, work from the Miller lab has shown that using a PLA to detect interactions between mitochondrial PTPIP51 and VAPB gives a semiquantitative measure of interactions between mitochondria and the ER (Stoica et al., 2016). To develop the PLA system as a tool to assess PO–ER associations, we first used the proteins we identified as known interactors and PO–ER tethers, ACBD5 and VAPB, as targets in the PLA (Figure 1(a)). Primary antibodies against ACBD5 (raised in rabbit) and VAPB (raised in mouse), which had previously been validated (Figure S1A-B; Costello, Castro, Camões, et al., 2017; Zhao et al., 2018), were used to perform a PLA in COS-7 cells. The individual antibodies generated minimal or zero PLA signals per cell (Figure 1(b), Panels I–III), but when both antibodies were used together, there was a significant increase in the

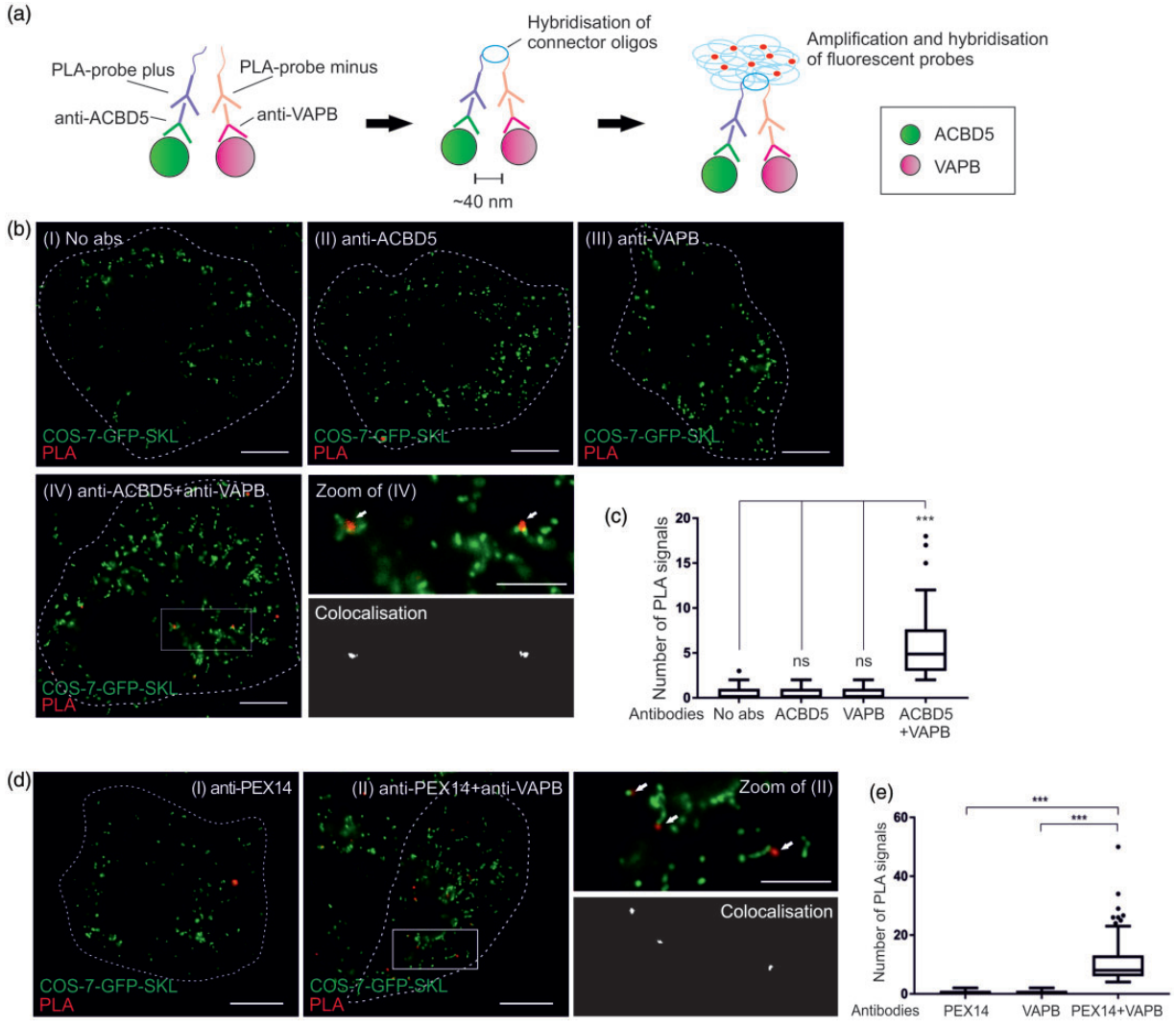

Figure 1. A PLA to assess peroxisome–ER associations. (a) Schematic overview of PLA method. (b) PLA performed on COS-7-GFP-SKL cells using (I) no antibody, (II) ACBD5 antibody only, (III) VAPB antibody only, and (IV) ACBD5 and VAPB antibodies combined. (c) Quantification of PLA signals per cell in (b) using the indicated antibodies. (d) PLA performed on COS-7-GFP-SKL cells using (I) PEX14 antibody only, (II) PEX14+VAPB antibodies. (e) Quantification of PLA signals per cell using the indicated antibodies. PLA signal is in red throughout with GFP-SKL (PTS1) as a peroxisomal marker (green). A one-way analysis of variance with Dunnett's multiple comparison test (c) and a two-tailed, unpaired *t* test (e) were used to determine statistical differences against the indicated group (***$p < .001$, *ns*: not significant). Thirty cells were used per condition, three repeats of each experiment. Scale bars: 10 μm. 5 μm in magnifications. Zooms are ×2.9 magnification of the white boxed area, with colocalized pixels from the green and red channels of the zoom area shown in white. PLA = proximity ligation assay; ACBD = acyl-CoA binding domain; VAPB = vesicle-associated membrane protein-associated protein-B.

number of PLA signals (Av = 5.6 ± 0.3 PLA signals per cell; Figure 1(b), panel IV) validating that both antibodies are required to generate a signal (quantified in Figure 1(c)). The PLA dots generated showed colocalization with the PO marker GFP-SKL (Figure 1(b), lower panels). As a negative control for antibody specificity, we also tested the ACBD5-VAPB PLA when no ACBD5 was present, in ACBD5 knockout (KO) HeLa cells. No PLA signal was observed in ACBD5 KO cells compared with wild-type controls (Figure S1C). As an additional negative control, we also tested antibodies against the peroxisomal matrix protein catalase and VAPB in HeLa cells but did not detect significant PLA signal.

To determine whether other peroxisomal membrane proteins could also be utilized in the PLA, we replaced the ACBD5 antibody in the assay with an antibody against the peroxisomal membrane protein PEX14. PEX14, ACBD5, and VAPB were recently identified, using a BioID approach, as interacting partners of an ER-targeted version of the long-chain acyl-CoA

synthetase ACSL1, suggesting PEX14 is in close proximity to the ER and may be a component of PO–ER contact sites (Young et al., 2018). Performing the PLA with a previously characterized (Grant et al., 2013) PEX14 antibody alone gave minimal signal (Figure 1(d), panel I), but both PEX14 and VAPB antibodies combined (Figure 1(d), Panel II) gave an average of 10.9 ± 0.8 PLA signals per cell (quantified in Figure 1(e)) which showed colocalization with the PO marker (Figure 1(d), inset panels). We speculate that the reason we observe slightly more signal in the PEX14-VAPB PLA than in the ACBD5-VAPB PLA may be due to differences in antibody specificity/avidity. Overall, although the number of PLA signals we observed was lower than might be expected, we next wanted to determine whether the PLA signal changed when PO–ER contacts are altered, which would suggest that the PLA could reliably give a semiquantitative readout of changes in PO–ER association.

Currently, the only known way to reduce PO–ER contacts is to modulate the levels of the tether components ACBD5 or VAPB. To confirm that our PLA system could measure reduced PO–ER associations, we utilized the PEX14-VAPB PLA to assess PO–ER associations in wild-type HeLa cells in comparison with ACBD5 KO HeLa cells (Ferdinandusse et al., 2016). We previously showed using EM that silencing of ACBD5 results in a decrease in PO–ER associations (Costello, Castro, Hacker, et al., 2017). To verify that our ACBD5 KO HeLa cells also showed reduced PO–ER contacts, we again employed EM and observed significant differences in PO–ER interactions (Figure 2(a)) with a reduction in both the number (Figure 2(b)) and the extent (Figure 2(c)) of PO–ER contacts in ACBD5 KO cells relative to wild-type cells. We then tested the same cells using the PEX14-VAPB PLA and detected a significant decrease in PLA signal in the ACBD5 KO cells compared with wild-type cells (Figure 2(d) and (e)). This suggests that the PLA is an effective way to measure the loss of PO–ER associations. To verify that changes in the PLA signal were not due to alterations in the levels of POs or peroxisomal proteins, we confirmed that both the levels of peroxisomal proteins (Figure 2(f)) and the number of POs (Figure 2(g)) were not altered when comparing wild-type and ACBD5 KO HeLa cells, and the levels of the proteins used in the PLA (VAPB and PEX14) were also not altered.

Previously, we have shown that overexpression of both ACBD5 and VAPB together results in an increase in PO–ER associations (Costello, Castro, Hacker, et al., 2017). To test whether this was also reflected in the PLA we overexpressed FLAG-ACBD5 and MYC-VAPB in COS-7 cells and then performed the PLA. Following FLAG-ACBD5 and MYC-VAPB coexpression (Figure S2A, Panel III), but not FLAG-ACBD5 overexpression alone (Figure S2A, Panel II), we observed a significant increase in PLA signal compared with untransfected controls (Figure S2A, Panel I), suggesting the PLA system is able to detect increases in interactions (Figure S2B). However, another interpretation of this result is that increasing the levels of the PLA targets might also increase PLA signal independent of the increased contacts. Thus, the decreased PLA signal we observed in ACBD5 KO HeLa cells compared with wild-type cells remains the strongest evidence that the PLA can be used to measure the changes in PO–ER contacts.

In our previous study, using EM, we observed that 60% to 70% of POs form close associations with the ER in COS-7 cells. However, this is not reflected in the PLA where we only see a small number of PLA signals. Relatively low number of PLA signals observed compared with the expected number of interactions is a phenomenon that has been discussed previously in another study comparing PLA with fluorescence resonance energy transfer (Mocanu, Váradi, Szöllosi, & Nagy, 2011). The authors noted that PLA allows the detection of only a fraction of the interacting proteins, as it not only depends on the proximity of the two proteins but also on the multiple downstream reactions, with steric hindrance from densely packed probes potentially having an inhibitory effect on the enzymes involved in the amplification process. Another phenomenon which we observed is that although the majority of PLA signals colocalize with, or are adjacent to, the peroxisomal marker (see Figure 1(b) and (d) and Figure S2A), there are occasional signals which do not colocalize. We assessed the extent of this colocalization and observed that ~80% of PLA dots overlapped with the PO marker (Figure S1D). These additional signals may represent nonspecific events or may potentially be due to heterogeneity in the peroxisomal population which has been previously reported (Schrader, Baumgart, Völkl, & Fahimi, 1994). In addition, it should be noted that the PLA remains a protein–protein interaction assay and as such can be impacted by protein modification events such as posttranslational modification of the partner proteins which could also impact on the PLA results, without necessarily altering interorganelle contacts.

Overall, we would suggest that our PO–ER PLA is suitable as a semiquantitative tool to measure the changes in contacts but not to assess the total number of organelle associations.

A Split-Fluorescence Reporter as a Measure of PO–ER Contacts

Another method that has recently been utilized to study the organelle associations is based on split-fluorescence systems. A dimerizable GFP (ddGFP; Alford et al., 2012) and a rapamycin-inducible FKBP-FRB

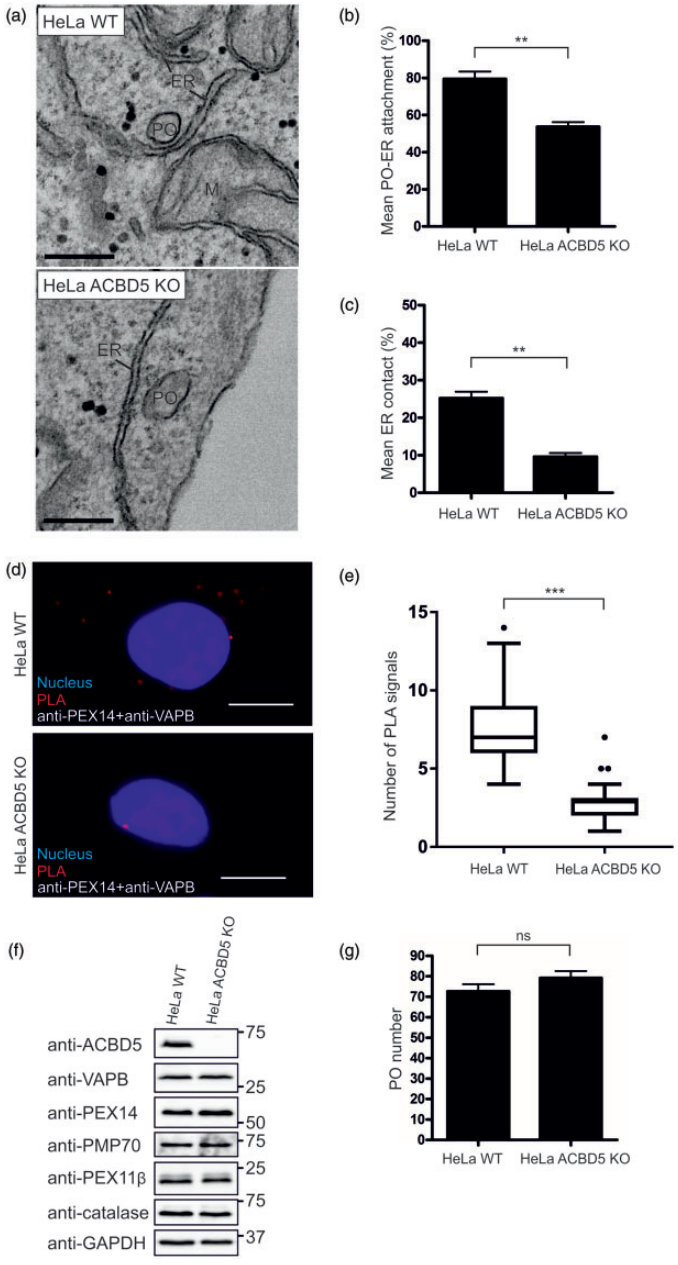

Figure 2. A reduction in PO–ER associations in ACBD5 KO HeLa cells can be detected using the PLA system. (a) Representative electron micrographs of PO–ER associations in WT and ACBD5 KO HeLa cells. (b) Quantitative analysis of the mean fraction of POs associated with the ER membrane in WT (Av = WT, 79.5 ± 3.9) and ACBD5 KO (Av = 53.7 ± 2.5) HeLa cells. (c) Assessment of the mean PO membrane surface in direct contact with the ER in WT (Av = WT, 25.2 ± 1.7) and ACBD5 KO (Av = 9.6 ± 1.0) HeLa cells. (d) PLA performed on WT and ACBD5 KO HeLa cells using PEX14 and VAPB antibodies. PLA signal in red, and nucleus in blue. (e) Quantification of PLA signals per cell in (d) using PEX14 and VAPB antibodies. (f) Immunoblots of cell lysates from WT and ACBD5 KO HeLa cells with the indicated antibodies against peroxisomal proteins (ACBD5, PEX14, PMP70, PEX11β, and catalase), VAPB and also GAPDH as a loading control. (g) Assessment of peroxisomal number in WT (Av = 72.7 ± 3.5) and ACBD5 KO (Av = 79.2 ± 3.6) HeLa cells. A two-tailed, unpaired *t* test was used to determine statistical differences against the indicated group (**$p < .01$. ***$p < .001$). Minimum 30 cells per condition, three repeats of each experiment. Scale bars: (a) 200 nm, (d) 10 μm. ER = endoplasmic reticulum; PO = peroxisome; M = mitochondrion; PLA = proximity ligation assay; WT = wild type; KO = knockout; ACBD = acyl-CoA binding domain; VAPB = vesicle-associated membrane protein-associated protein-B.

heterodimerization (Csordás et al., 2010) system have been generated to assess mitochondria–ER associations. More recently, an spGFP system has been employed to measure the mitochondria–ER associations (Cieri et al., 2018). We initially trialed a ddGFP system but observed poor signal to noise ratio using this approach. Instead, we sought to modify the spGFP system to allow the study of PO–ER associations and redesigned the spGFP moieties to contain ER and peroxisomal targeting signals. These were generated by fusing the transmembrane domain and tail (TMD-T) region of ACBD5 and VAPB to the split GFP moieties spGFP1-10 and spGFP11, respectively (Figure 3(a)). We and others have previously shown that the TMD-T of ACBD5 and VAPB are sufficient to target fluorescent proteins to the peroxisomal and ER membrane, respectively (Costello, Castro, Camões, et al., 2017; Harmon, Larkman, Hardingham, Jackson, & Skehel, 2017; Teuling et al., 2007). Initially, by cotransfecting an untargeted cytosolic spGFP portion with the corresponding ER or PO targeted spGFP portion, we showed that targeting of the individual spGFP moieties was as expected (Figure 3(b)). The untargeted spGFP portions give cytosolic signal when expressed together (Figure 3(b), panel I), but we observe characteristic ER staining (Figure 3(b), Panel II) when untargeted spGFP1-10 is expressed with spGFP11-VAPB and observe punctate peroxisomal staining when untargeted KATEβ11 is expressed with spGFP1-10-ACBD5 (Figure 3(b), Panel III). Individually, the spGFP1-10 and spGFP11 portions did not fluoresce, but when plasmids encoding spGFP1-10-ACBD5 and spGFP11-VAPB were cotransfected, we observed a punctate green signal, which colocalized with the peroxisomal marker Pex14 (Figure 3(c) and (d)). A comparison of the number of spGFP and PEX14 signals per cell suggests that ~65% of POs are in close contact with the ER (Figure 3(e)), which supports previous EM data (Costello, Castro, Hacker, et al., 2017). This suggested that this system could be a useful measure of PO–ER associations.

One potential problem that has been highlighted with split-fluorescence systems is the reversibility, although previous reports on the mitochondria–ER system suggested that spGFP may be reversible (Yang et al., 2018). As we previously validated that the PLA can measure increases in PO–ER contacts, we used the PLA on COS-7 cells expressing the spGFP PO–ER reporter (note that the ACBD5 and VAPB antibodies will not recognize the ACBD5 and VAPB TMD-T region in the spGFP reporters and also that the TMD-T regions of ACBD5 and VAPB do not interact with each other so cannot tether in this way). Interestingly, we observed an increase in PLA signal following transfection of the spGFP PO–ER reporter, suggesting expression of these constructs was increasing PO–ER associations (Figure 3(f) and (g)). To further explore this, we also expressed the spGFP reporter system in wild-type and ACBD5 KO HeLa cells and compared the number of spGFP signals. Previously, we were able to observe using both the EM and the PLA a reduced number of PO–ER interactions in ACBD5 KO HeLa cells. However, using the spGFP system, we did not observe a significant difference between the numbers of spGFP signals in wild-type cells compared with ACBD5 KO cells (Figure S2C and D). This implies that although the spGFP tool is able to label sites of PO–ER associations, it should be treated with caution as the reporter itself may act as an artificial tether and increase organelle contacts. While this result suggests that the spGFP reporter is acting as a tether, it may also reflect the nature of the PO–ER interaction which appears to be different to mitochondria–ER interactions. EM studies have routinely observed a wrapping of entire peroxisomal structure with fenestrated ER (see schematic example in Figure 3(h)), and it is possible that this type of interaction is artificially stabilized by expressing the spGFP PO–ER reporters. The reversibility of the split-fluorescent systems is the topic of some debate in the field and whether or not this occurs may depend on the affinity of the two portions of GFP for each other versus the affinity of the formation and collapse of the contact sites between the organelles. Presumably, these values will vary for different organelles and likely depend on the affinities of endogenous tethers; for PO–ER contacts, this is currently unknown. Previous studies have suggested that spGFP reporters are to some extent reversible and are suitable for measurement of mitochondria–ER contacts (Yang et al., 2018), in particular the *Deinococcus radiodurans* infrared fluorescent protein IFP1.4 system has been successfully utilized for organelle proximity measurements without inducing tethering (Shai et al., 2018; Tchekanda, Sivanesan, & Michnick, 2014). However, the earlier observations indicate that the spGFP may not be useful for the quantification of PO–ER contacts.

Spatial Analysis of PO–ER Contacts in MFF-Deficient Fibroblasts Suggests the ER Is Enriched Around the Peroxisomal Body

Having developed new light microscopy-based methods to study PO–ER contacts, we now wanted to use these techniques, in combination with our existing EM method, to test our previously proposed model on how POs and the ER interact to facilitate peroxisomal biogenesis (Costello & Schrader, 2018). POs can form and multiply out of preexisting POs by membrane growth and division. This multistep process involves membrane deformation and elongation of a preexisting (mother) PO, constriction of the elongated membrane and final membrane scission

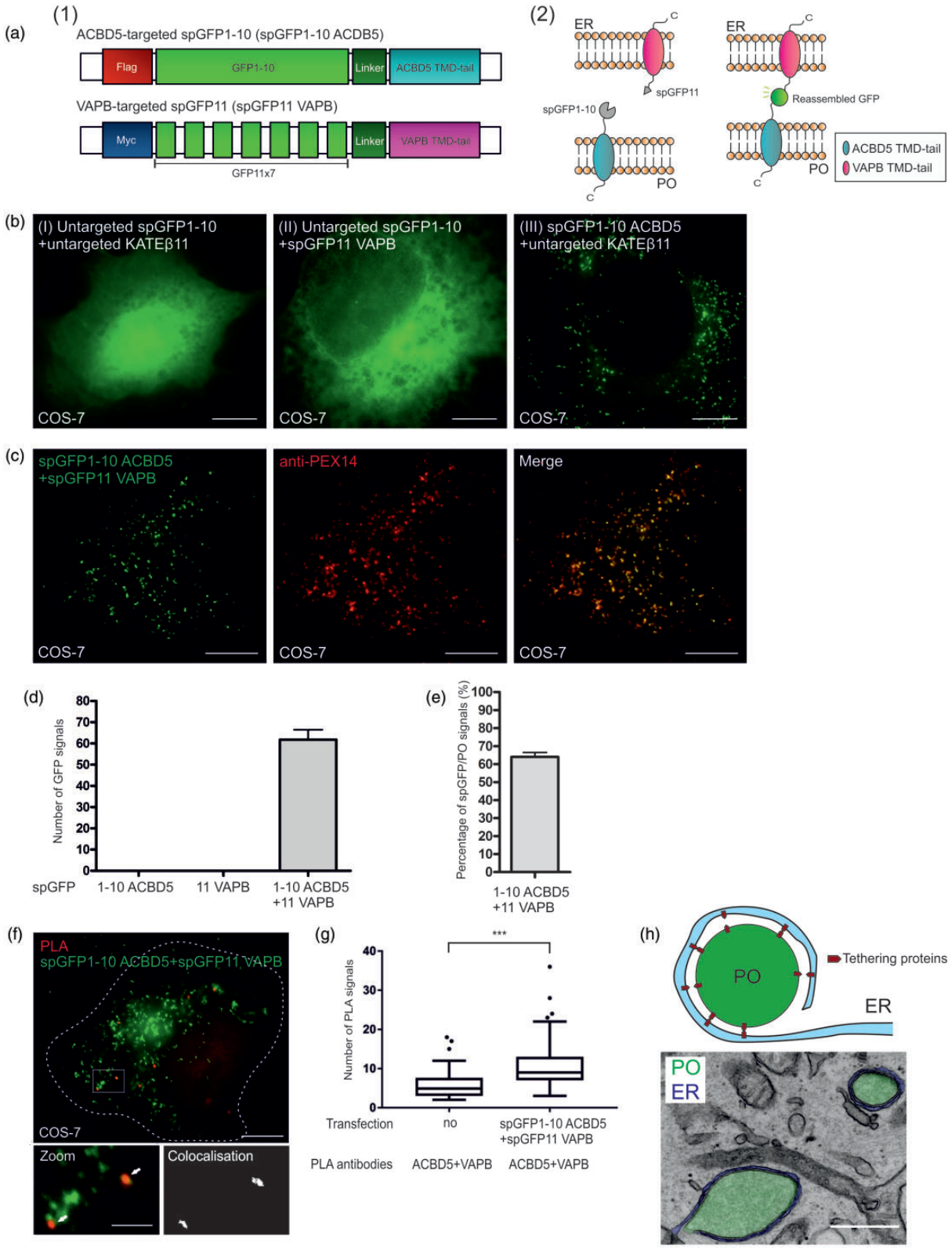

Figure 3. An spGFP assay to measure PO–ER associations. (a) (1) Overview of spGFP constructs. (2) Schematic overview of the spGFP system used to measure the PO–ER associations. (b) COS-7 cells transfected with the indicated plasmids to show localization of the spGFP11-VAPB and spGFP1-10-ACBD5 to the ER and POs, respectively, (I) untargeted KATEβ11 and spGFP1-10 as controls, (II) untargeted spGFP1-10 with spGFP11-VAPB, and (III) untargeted KATEβ11 with spGFP1-10-ACBD5. (c) COS-7 cells cotransfected with

by recruitment of the dynamin-related fission GTPase Drp1 through membrane adaptors such as MFF or Fis1 (Schrader et al., 2015). Peroxisomal membrane elongation requires phospholipids, which are delivered by a nonvesicular mechanism (Raychaudhuri & Prinz, 2008). We recently demonstrated that ACBD5-VAPB-mediated PO–ER contacts are required for peroxisomal membrane expansion, suggesting a role for these contacts in lipid transfer from the ER to POs (Costello, Castro, Hacker, et al., 2017). These findings also explain why POs in cells with a defect in PO division are highly elongated; they constantly receive lipids from the ER and elongate but are unable to divide (Castro et al., 2018; Costello & Schrader, 2018). In support of this model, we recently demonstrated that loss of ACBD5 in MFF-deficient fibroblasts reduced peroxisomal membrane expansion, whereas expression of an artificial PO–ER tether restored the highly elongated PO morphology or induced hyperelongation (Costello, Castro, Hacker, et al., 2017). In this model, a spherical "mother" PO is tethered to the ER, giving rise to tubular extensions which elongate before being divided by the Drp1-dependent fission machinery (Figure 4(a)). To test if tethering does indeed occur at the spherical body of the "mother" PO or if contacts with the ER are equally distributed along the tubular extensions, we expressed the spGFP PO–ER reporter system in MFF-deficient fibroblasts. In these cells, division-incompetent POs form highly elongated tubules stemming from a spherical peroxisomal body (Costello, Castro, Hacker, et al., 2017; see example in Figure 4(b)). We first tested the localization of the individual spGFP moieties to assess their localization in MFF-deficient fibroblasts using the untargeted Kateβ11 and spGFP1-10. The PO-targeted spGFP1-10-ACBD5 fusion alone labeled both the tubules and the spherical POs when expressed in MFF-deficient fibroblasts, while the spGFP11-VAPB showed an ER-like staining (Figure 4(c)). However, when spGFP1-10-ACBD5 and spGFP11-VAPB were expressed together, the GFP signal was concentrated at the spherical peroxisomal structures (which give rise to the tubular extensions), with occasional, but much weaker signals at the tubules (Figure 4(d)). This suggests that PO–ER associations are not equally distributed along the membrane tubules but are most prevalent at the spherical bodies. To further explore this, we performed EM on untransfected MFF-deficient fibroblasts (Figure 4(e)). Similar to the spGFP results, using EM, we observed that the ER did not distribute evenly along the tubules, but was rather frequently observed to decorate a distal region, which we suggest may represent the tubule-forming peroxisomal body. In rare occasions, the ER was found associated with regions along the length of the tubule (Figure 4(e), lower left panel). These ER-associated regions were larger in diameter than the tubular extensions and may represent peroxisomal bodies which form extensions in two directions.

These observations suggest that the ER predominantly associates with the peroxisomal body in our cell model. In support of our findings, it should also be noted that endogenous ACBD5 is also mainly located at the spherical PO body in MFF-deficient cells (Costello, Castro, Hacker, et al., 2017). Based on this, we speculate that the peroxisomal body may represent the major PO–ER interface, which allows phospholipid transfer for peroxisomal membrane expansion (prior to division/multiplication in wild-type cells).

In summary, we have developed two novel techniques to measure the PO–ER interactions, based on the PLA and spGFP systems. The PLA can be used with either ACBD5 or PEX14 as peroxisomal targets and VAPB as an ER target and is capable of measuring changes in PO–ER interactions, as evidenced by modulation of known tethering components. As ACBD5, PEX14, and VAPB are found in a wide variety of cell types, this assay should be widely applicable as a valid measure of changes in endogenous PO–ER associations, which does not require specialist knowledge or equipment. As knowledge on contact site components increases and new antibodies become available, these could also be utilized in PLAs. The spGFP system has the

Figure 3. Continued.
plasmids encoding the spGFP11-VAPB and spGFP1-10-ACBD5, stained with PEX14 (red) as a peroxisomal marker. (d) Quantification of the average number of GFP signals generated with the spGFP constructs transfected individually (no signal) or when combined (Av = 61.8 GFP signals per cell ± 4.7). (e) Quantification of the number of spGFP signals per PO, assessed as the total number of spGFP signals/the total number of Pex14 signals per cell (Av = 64.0 ± 2.5). (f) PLA using ACBD5 and VAPB antibodies on COS-7 cells transfected with plasmids encoding the spGFP11-VAPB and spGFP1-10-ACBD5. PLA signals in red. Zooms are ×3.9 magnification of the white boxed area. Colocalized pixels from the green and red channels of the zoom area are shown in white. (g) Quantification of PLA signals per cell using ACBD5 and VAPB antibodies in COS-7 cells, comparing PLA signals in untransfected cells versus cells cotransfected with the spGFP reporter. (h) Schematic illustration of PO–ER interactions showing extent of ER wrapping and example electron micrograph, with false coloring, of POs in MFF-deficient fibroblasts showing extensive ER wrapping. A two-tailed, unpaired *t* test was used to determine statistical differences against the indicated group (***$p < .001$). Thirty cells per condition, three repeats of each experiment. Scale bars: 10 μm in (b), (c), and (f) and 0.5 μm in (h), higher magnification view in (f) is 2.5 μm. ER = endoplasmic reticulum; PO = peroxisome; GFP = green fluorescent protein; spGFP = split superfolder GFP; PLA = proximity ligation assay; TMD-tail = transmembrane domain and tail; ACBD = acyl-CoA binding domain; VAPB = vesicle-associated membrane protein-associated protein-B.

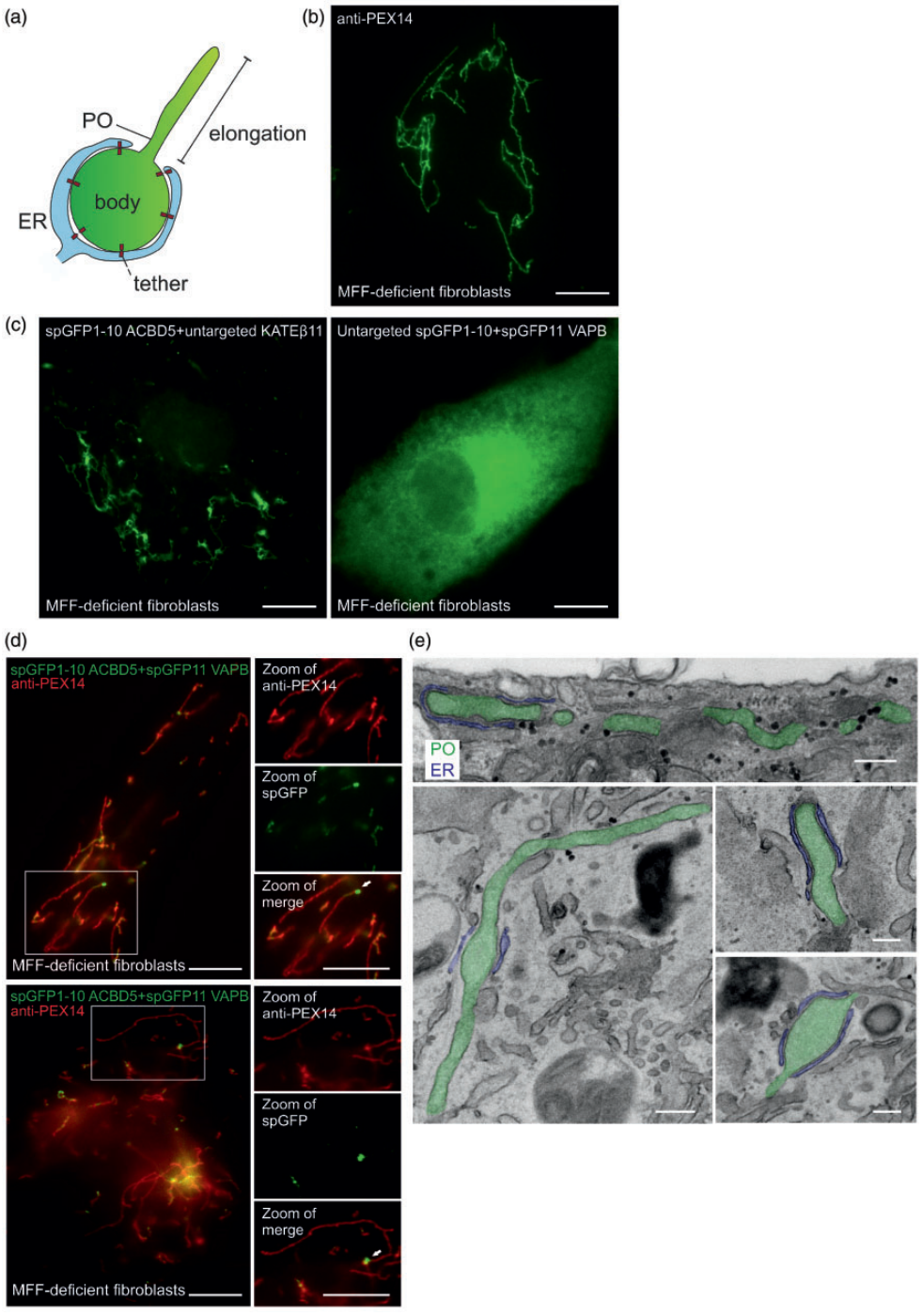

Figure 4. spGFP reporter and electron microscopy analysis suggests that PO–ER contacts are most prevalent at the spherical peroxisomal body. (a) Model of the location of PO–ER tethers during peroxisomal elongation. (b) Representative example of elongated POs in MFF-deficient fibroblasts labeled with anti-PEX14 antibody as a peroxisomal marker. (c) Expression of spGFP1-10-ACBD5 with untargeted Kateβ11 and spGFP-11-VAPB with untargeted spGFP1-10 in MFF-deficient fibroblasts showing peroxisomal and ER localization respectively. (d) Representative images of spGFP PO–ER reporter in MFF-deficient fibroblasts, labeled with anti-PEX14 in red as peroxisomal marker. Zooms are ×1.3 magnification of the white boxed area. (e) Representative electron micrographs, with false coloring, of PO–ER associations in untransfected MFF-deficient fibroblasts showing ER contacts are not evenly distributed along peroxisomal tubules but are focused primarily around the distal ends of POs and can occasionally be found at internal, expanded, regions within a tubule. PO = peroxisome (green); ER = endoplasmic reticulum (blue). Scale bar: 10 μm in (b), (c), and (d) and 0.2 μm in (e). GFP = green fluorescent protein; spGFP = split superfolder GFP; ACBD = acyl-CoA binding domain; VAPB = vesicle-associated membrane protein-associated protein-B.

advantage that it can be used for live cell imaging, but the disadvantage that it may impact on the tethering process. We also observed occasional mistargeting of the spGFP1-10-ACBD5 portion of the spGFP when expression levels were very high, in line with previous observations of ACBD5 mistargeting (Costello, Castro, Camões, et al., 2017). However, we were still able to use this system to provide information on PO–ER associations. Overall, we would suggest that the PLA can be a useful tool to measure the PO–ER interactions, taking into consideration the caveats discussed earlier. As noted in a recent review article (Scorrano et al., 2019), it is highly advisable to utilize multiple methods, combining biochemical and fluorescent techniques with EM approaches to assess contact sites. The advantages and disadvantages of the PLA and spGFP systems techniques are summarized and compared with EM in Table 1.

Materials and Methods

Plasmids

The spGFP PO–ER reporter constructs were based on the original system (Kamiyama et al., 2016). The TMD-T regions of ACBD5 (residues 503-534) and VAPB (residues 223-243) were inserted downstream of one copy of spGFP1-10 or seven copies of spGFP11X7, respectively, with a 17 amino acid linker (GTGGGGS GTGGGGSGGG) between the spGFP and the TMD-T and a 15 amino acid linker between the repeats in spGFP11. To facilitate the detection of the spGFP halves, FLAG or MYC tags were cloned upstream of the spGFP1-10 and spGFP11, respectively. These constructs were generated by gene synthesis (Eurofins) and then subcloned into pcDNA3.1 (+) as HindIII-XhoI fragments. See Figure 3(a) for schematic. Untargeted KATEβ11 and spGFP1-10 control plasmids were kind gifts from T. Cali (Universita degli studi Di Padova, Italy; Cieri et al., 2018). MYC-VAPB was a generous gift from C. Miller (King's College London, London, UK). FLAG-ACBD5 was previously described (Costello, Castro, Hacker, et al., 2017).

Antibodies

PLA: Anti-ACBD5 rabbit antibody (HPA012145; Sigma-Aldrich), anti-PEX14 rabbit antibody (Grant et al., 2013; generated by D. Crane, Griffith University, Brisbane, Australia), and anti-VAPB mouse antibody (66191-1-Ig; Proteintech) were used. Immunoblots: Anti-ACBD5, PEX14, and VAPB as earlier; anti-PMP70 (SAB4200181; Sigma); anti-PEX11β (ab 182100; Abcam); anti-Catalase (ab179843; Abcam); and anti-GAPDH (ProSci) were used.

Cell Culture and Transfection

COS-7 (CRL-1651; ATCC), COS-7-GFP-SKL (stably transfected with PO-targeted GFP-SKL [SKL is a PO targeting signal PTS1]; Koch, Schneider, Lüers, & Schrader, 2004), HeLa and ACBD5 KO HeLa (generated by J. Koster, Univ. of Amsterdam, Netherlands; Ferdinandusse et al., 2016), and MFF-deficient fibroblasts (kindly provided by F. S. Alkuraya, King Faisal Specialist Hospital and Research Center, Riyadh, Saudi Arabia; Koch et al., 2016; Shamseldin et al., 2012) were cultured in Dulbecco's Modified Eagle Medium (DMEM) high glucose (4.5 g/L) supplemented with 10% (v/v) fetal bovine serum, 100 U/ml penicillin, and 100 μg/ml streptomycin at 37°C with 5% CO_2 and 95% humidity. COS-7 cells and MFF-deficient fibroblasts were transfected using diethylaminoethyl-dextran or microporation, respectively, as previously described (Costello, Castro, Hacker, et al., 2017).

Table 1. Advantages and Disadvantages of the PLA, spGFP Reporter and EM Systems for Assessing Peroxisome–Endoplasmic Reticulum Interactions.

	PLA	spGFP reporter	EM
Suitable for fixed cells?	Y	Y	Y
Suitable for live cell imaging?	N	Y	N
Requires transfection?	N	Y	N
Requires specific antibodies?	Y	N	N
Representative of the number of organelle interactions?	N	N	Y
Potential for the method to cause alterations to organelles?	N	Y	N
May be altered by posttranslational modifications?	Y	N	N
Potential for high-throughput assays?	Y	Y	N
Possibility to measure the changes in contact site size?	N	Y	Y

Note. Y = yes; N = no; GFP = green fluorescent protein; spGFP = split superfolder GFP; PLA = proximity ligation assay; EM = electron microscopy.

Proximity Ligation Assay

For the PLA, 90,000 cells were seeded onto a 3.5-cm diameter cell view dish (Greiner BioOne). PLA was performed using Duolink® PLA Red kit (Sigma-Aldrich) according to the manufacture's protocol. In short, cells were fixed with 4% (v/v) paraformaldehyde for 20 min, at 24 hr (HeLa) or 48 hr after seeding, and permeabilized with 0.2% (v/v) Triton X-100 for 10 min. After 3 times washing with phosphate-buffered saline (PBS), cells were incubated with blocking buffer for 30 min at 37°C. Cells were then incubated with 50 µL primary antibodies for 1 hr at room temperature. Anti-ACBD5 antibody (1:100), anti-PEX14 (1:1,400), and anti-VAPB antibody (1:200) were used. Cells were washed with Duolink Wash Buffer A twice and incubated with 40 µL PLA probe solution including PLA probe anti-rabbit plus and anti-mouse minus for 1 hr at 37°C. Cells were then washed with Duolink Wash Buffer A twice and incubated with ligase for 30 min at 37°C. After washing with Duolink Wash Buffer A again, polymerase was added for amplification and incubated for 100 min at 37°C. Finally, cells were washed with Duolink Wash Buffer B for 10 min twice and 0.01× Buffer B for 1 min with shading. Nuclei were stained with Hoechst 33258 (Polysciences), and samples were then mounted on a 19 mm ø coverslip using Mowiol with n-propyl gallate as an antifading reagent (Schrader et al., 1998). In general, we suggest stringent washing and avoid drying the cell view dish by always covering with humid paper towel during incubation.

Immunoblotting

HeLa cells were washed in PBS and then lysed by mixing with ice-cold lysis buffer (25 mM Tris-HCl, pH 7.5, 150 mM NaCl, 1% Nonidet P-40, 1 mM phenylmethylsulfonyl fluoride, and protease inhibitor cocktail) for 30 min at 4°C. Undissolved material was pelleted by centrifugation at 15,000g. After normalizing protein concentration, total lysates were mixed with Laemli buffer and analyzed by Western immunoblotting, with semidry transfer. Enhanced chemiluminescence (ECL) signals were detected using the G-Box Chemi (Syngene).

spGFP Assays

For the spGFP assay, 250,000 COS-7 cells were seeded onto 19 mm ø coverslips in a 6 cm ø dish the day before transfection. 3.3 µg spGFP1-10-ACBD5 and spGFP11-VAPB or as a control, untargeted spGFP1-10 and a β11-tagged RFP (KATEβ11) plasmids were transfected into the cells; 48 hr after transfection, cells were processed for immunofluorescence. Briefly, cells were fixed with 4% paraformaldehyde in PBS (pH 7.4), permeabilized with 0.2% Triton X-100, and incubated with antibodies as described previously (Schrader, Islinger, & Schrader, 2017). Cells were stained with the peroxisomal membrane marker anti-PEX14.

Microscopy

Cells were observed using an Olympus IX81 microscope (Olympus) equipped with an UPlanSApo 100×/1.40 oil objective (Olympus) and a CoolSNAP HQ2 CCD camera. Digital images were taken and processed using VisiView software (Visitron Systems). Images were adjusted for contrast and brightness using MetaMorph 7 (Molecular Devices). Analyses were performed on rendered *z*-stacks and single-plane images. As COS-7 cells are very flat, single-plane analysis gave very similar results (e.g., PO–ER contacts with anti-ACBD5/VAPB antibodies; PLA signal *z*-stack: 11.31 ± 0.5; single: 10.4 ± 0.4; $n = 91$ cells) and was used in the following to increase throughput. EM was performed essentially as previously described (Costello, Castro, Hacker, et al., 2017). In brief, monolayers of cells were fixed for 1 hr in 0.5% glutaraldehyde in 0.2M PIPES buffer (pH 7.2) and postfixed in 1% osmium tetroxide (reduced with 1.5% w/v potassium ferrocyanide) in cacodylate buffer for 1 hr. After washing in deionized water, the cells were dehydrated in a graded ethanol series before embedding in Durcupan resin (Sigma-Aldrich); 60 nm ultra-thin sections were collected on pioloform-coated 100 mesh copper EM grids (Agar Scientific) and contrasted with lead citrate prior to imaging using a JEOL JEM 1400 transmission electron microscope operated at 120 kV. Images were taken with a digital camera (ES 1000W CCD, Gatan). Quantification of PO–ER contacts was performed as previously (Costello, Castro, Hacker, et al., 2017), In brief, POs were sampled ($n = 48$–64 POs per experimental grid) by scanning the EM grids systematic uniform random. To estimate the mean fraction of total PO membrane surface in direct contact with the ER, a stereological approach by line intersection counting was used. Intersections were classified as direct membrane contact (defined as "attachment") if there was <15 nm distance between PO and ER membranes.

Statistical Analyses

Quantification of PLA fluorescent signals was performed using ImageJ software, using a custom macro which utilized the analyze particles function, following manual thresholding. To analyze PLA colocalization with PEX14 marker, following image processing colocalization was visualized as white pixels using an ImageJ "Colocalization" plugin (Bourdoncle, 2004). Quantification was performed by manually counting the number of PLA dots with and without white

pixels. Statistical analysis was performed using GraphPad Prism Version 7 (GraphPad Software). All experiments for quantification were performed with at least three independent repeats and a minimum of 90 cells were observed per condition. In box whisker plots, the plots show outliers calculated by the Tukey's method. Center lines are median values and boxes extend from the 25th to the 75th percentile of each group's distribution of values, vertical extending lines mean adjacent values. Error bars shown are standard error of the mean. A one-way analysis of variance with Dunnett's multiple comparison test or a two-tailed, unpaired *t* test was used to determine statistical differences against the indicated group (**$p < .01$; ***$p < .001$).

Acknowledgments

The authors thank all colleagues who provided cell lines, plasmids, and antibodies and Ana Correia for support with embedment and sectioning for electron microscopy.

Author Contributions

AB, MK, JBP, CH, and TS performed the experiments. AB, MK, JBP, CH, and JLC analyzed the data and generated the figures; JLC and MS conceived the project and wrote the manuscript; all authors contributed to methods.

Declaration of Conflicting Interests

The author(s) declared no potential conflicts of interest with respect to the research, authorship, and/or publication of this article.

Funding

The author(s) disclosed receipt of the following financial support for the research, authorship, and/or publication of this article: This work was supported by Biotechnology and Biological Sciences Research Council (BB/N01541X/1; to M. S.) and H2020-MSCA-ITN-2018 812968 PERICO (M. S., H. R. W.); A. B. was supported by a University of Exeter CLES Research Internship scheme (SCP 3885); M. K. was supported by the Japan Society for the Promotion of Science; and J. B. P. was supported by Zellweger UK, The Sidney Perry Foundation, and The Devon Educational Trust. The research data supporting this publication are provided within this article.

ORCID iD

Alexa Bishop https://orcid.org/0000-0002-7013-7884 Josiah B. Passmore https://orcid.org/0000-0001-7791-3439 Joseph L. Costello https://orcid.org/0000-0002-2867-1864

References

Alford, S. C., Ding, Y., Simmen, T., & Campbell, R. E. (2012). Dimerization-dependent green and yellow fluorescent proteins. *ACS Synthetic Biology*, *1*, 569–575.

Alpy, F., Rousseau, A., Schwab, Y., Legueux, F., Stoll, I., Wendling, C., … Levine, T. P. (2013). STARD3 or STARD3NL and VAP form a novel molecular tether between late endosomes and the ER. *Journal of Cell Science*, *126*, 5500–5512.

Bourdoncle, P. (2004). *ImageJ "Colocalization" plugin*. Paris, France: Institut Jacques Monod, Service Imagerie. Retrieved from https://imagej.nih.gov/ij/plugins/colocalization.html

Castro, I. G., Richards, D. M., Metz, J., Costello, J. L., Passmore, J. B., Schrader, T. A., … Schrader, M. (2018). A role for Mitochondrial Rho GTPase 1 (MIRO1) in motility and membrane dynamics of peroxisomes. *Traffic*, *19*, 229–242.

Cieri, D., Vicario, M., Giacomello, M., Vallese, F., Filadi, R., Wagner, T., … Calì, T. (2018). SPLICS: A split green fluorescent protein-based contact site sensor for narrow and wide heterotypic organelle juxtaposition. *Cell Death & Differentiation*, *25*, 1131–1145.

Cohen, S., Valm, A. M., & Lippincott-Schwartz, J. (2018). Interacting organelles. *Current Opinion in Cell Biology*, *53*, 84–91.

Costello, J. L., Castro, I. G., Camões, F., Schrader, T. A., McNeall, D., Yang, J., … Ribeiro, D. (2017). Predicting the targeting of tail-anchored proteins to subcellular compartments in mammalian cells. *Journal of Cell Science*, *130*, 1675–1687.

Costello, J. L., Castro, I. G., Hacker, C., Schrader, T. A., Metz, J., Zeuschner, D., … Manner, A. (2017). ACBD5 and VAPB mediate membrane associations between peroxisomes and the ER. *Journal of Cell Biology*, *216*, 331–342.

Costello, J. L., Castro, I. G., Schrader, T. A., Islinger, M., & Schrader, M. (2017). Peroxisomal ACBD4 interacts with VAPB and promotes ER-peroxisome associations. *Cell Cycle*, *16*, 1039–1045.

Costello, J. L., & Schrader, M. (2018). Unloosing the Gordian knot of peroxisome formation. *Current Opinion in Cell Biology*, *50*, 50–56.

Csordás, G., Várnai, P., Golenár, T., Roy, S., Purkins, G., Schneider, T. G., … Hajnóczky, G. (2010). Imaging interorganelle contacts and local calcium dynamics at the ER–mitochondrial interface. *Molecular Cell*, *39*, 121–132.

Eisenberg-Bord, M., Shai, N., Schuldiner, M., & Bohnert, M. (2016). A tether is a tether is a tether: Tethering at membrane contact sites. *Developmental Cell*, *39*, 395–409.

Ferdinandusse, S., Falkenberg, K. D., Koster, J., Mooyer, P. A., Jones, R., van Roermund, C. W. T., … Waterham, H. R. (2016). ACBD5 deficiency causes a defect in peroxisomal very long-chain fatty acid metabolism. *Journal of Medical Genetics*, *54*, 330–337.

Friedman, J. R., Lackner, L. L., West, M., DiBenedetto, J. R., Nunnari, J., & Voeltz, G. K. (2011). ER tubules mark sites of mitochondrial division. *Science*, *334*, 358–362.

Gatta, A. T., & Levine, T. P. (2017). Piecing together the patchwork of contact sites. *Trends in Cell Biology*, *27*, 214–229.

Grant, P., Ahlemeyer, B., Karnati, S., Berg, T., Stelzig, I., Nenicu, A., … Baumgart-Vogt, E. (2013). The biogenesis protein PEX14 is an optimal marker for the identification

and localization of peroxisomes in different cell types, tissues, and species in morphological studies. *Histochemistry and. Cell Biology*, *140*, 423–442.

Harmon, M., Larkman, P., Hardingham, G., Jackson, M., & Skehel, P. (2017). A bi-fluorescence complementation system to detect associations between the endoplasmic reticulum and mitochondria. *Scientific Reports*, *7*, 17467.

Helle, S. C. J., Kanfer, G., Kolar, K., Lang, A., Michel, A. H., & Kornmann, B. (2013). Organization and function of membrane contact sites. *Biochimica et Biophysica Acta (BBA)-Molecular Cell Research*, *1833*, 2526–2541.

Hua, R., Cheng, D., Coyaud, É., Freeman, S., Di Pietro, E., Wang, Y., … Brumell, J. H. (2017). VAPs and ACBD5 tether peroxisomes to the ER for peroxisome maintenance and lipid homeostasis. *Journal of Cell Biology*, *216*, 367–377.

Kakimoto, Y., Tashiro, S., Kojima, R., Morozumi, Y., Endo, T., & Tamura, Y. (2018). Visualizing multiple inter-organelle contact sites using the organelle-Targeted split-GFP system. *Scientific Reports*, *8*, 6175.

Kamiyama, D., Sekine, S., Barsi-Rhyne, B., Hu, J., Chen, B., Gilbert, L. A., … Huang, B. (2016). Versatile protein tagging in cells with split fluorescent protein. *Nature Communications*, *7*, 11046.

Koch, A., Schneider, G., Lüers, G. H., & Schrader, M. (2004). Peroxisome elongation and constriction but not fission can occur independently of dynamin-like protein 1. *Journal of Cell Science*, *117*, 3995–4006.

Koch, J., Feichtinger, R. G., Freisinger, P., Pies, M., Schrödl, F., Iuso, A., … Haack, T. B. (2016). Disturbed mitochondrial and peroxisomal dynamics due to loss of MFF causes Leigh-like encephalopathy, optic atrophy and peripheral neuropathy. *Journal of Medical Genetics*, *4*, 270–278.

Lewis, S. C., Uchiyama, L. F., & Nunnari, J. (2016). ER–mitochondria contacts couple mtDNA synthesis with mitochondrial division in human cells. *Science*, *353*, aaf5549.

Mocanu, M. M., Váradi, T., Szöllosi, J., & Nagy, P. (2011). Comparative analysis of fluorescence resonance energy transfer (FRET) and proximity ligation assay (PLA). *Proteomics*, *11*, 2063–2070.

Novikoff, P. M., & Novikoff, A. B. (1972). Peroxisomes in absorptive cells of mammalian small intestine. *Journal of Cell Biology*, *53*, 532–60.

Raychaudhuri, S., & Prinz, W. A. (2008). Nonvesicular phospholipid transfer between peroxisomes and the endoplasmic reticulum. *Proceedings of the National Academy of Sciences of the United States of America*, *105*, 15785–15790.

Rizzuto, R., Pinton, P., Carrington, W., Fay, F. S., Fogarty, K. E., Lifshitz, L. M., … Pozzan, T. (1998). Close contacts with the endoplasmic reticulum as determinants of mitochondrial Ca2+ responses. *Science*, *280*, 1763–1766.

Schrader, M., Baumgart, E., Völkl, A., & Fahimi, H. D. (1994). Heterogeneity of peroxisomes in human hepatoblastoma cell line HepG2. Evidence of distinct subpopulations. *European Journal of Cell Biology*, *64*, 281–294.

Schrader, M., Costello, J. L., Godinho, L. F., Azadi, A. S., & Islinger, M. (2015). Proliferation and fission of peroxisomes—An update. *Biochimica et Biophysica Acta (BBA)-Molecular Cell Research*, *1863*, 971–983.

Schrader, M., Godinho, L. F., Costello, J. L., & Islinger, M. (2015). The different facets of organelle interplay—An overview of organelle interactions. *Frontiers in Cell and Developmental Biology*, *3*, 56.

Schrader, M., Kamoshita, M., & Islinger, M. (2019). Organelle interplay–peroxisome interactions in health and disease. *Journal of Inherited Metabolic Disease*. doi:10.1002/jimd.12083

Schrader, M., Reuber, B. E., Morrell, J. C., Jimenez-sanchez, G., Obie, C., Stroh, T. A., … Gould, S. J. (1998). Expression of PEX11β mediates peroxisome proliferation in the absence of extracellular stimuli. *Journal of Biological Chemistry*, *273*, 29607–29614.

Schrader, T. A., Islinger, M., & Schrader, M. (2017). Detection and immunolabeling of peroxisomal proteins. *Methods in Molecular Biology*, *1595*, 113–130.

Scorrano, L., De Matteis, M., Emr, S. D., Giordano, F., Hajnóczky, G., Kornmann, B., … Rizzuto, R. (2019). Coming together to define membrane contact sites. *Nature Communications*, *10*, 1287.

Shai, N., Yifrach, E., Van Roermund, C. W. T., Cohen, N., Bibi, C., Ijlst, L., … Mari, M. C. (2018). Systematic mapping of contact sites reveals tethers and a function for the peroxisome–mitochondria contact. *Nature Communications*, *9*, 1761.

Shamseldin, H. E., Alshammari, M., Al-Sheddi, T., Salih, M. A., Alkhalidi, H., Kentab, A., … Alkuraya, F. S. (2012). Genomic analysis of mitochondrial diseases in a consanguineous population reveals novel candidate disease genes. *Journal of Medical Genetics*, *49*, 234–241.

Söderberg, O., Gullberg, M., Jarvius, M., Ridderstråle, K., Leuchowius, K. J., Jarvius, J., … Landegren, U. (2006). Direct observation of individual endogenous protein complexes *in situ* by proximity ligation. *Natre Methods*, *3*, 995–1000.

Stoica, R., Paillusson, S., Gomez-Suaga, P., Mitchell, J. C., Lau, D. H., Gray, E. H., … Hanger, D. P. (2016). ALS/FTD-associated FUS activates GSK-3β to disrupt the VAPB–PTPIP51 interaction and ER–mitochondria associations. *EMBO Reports*, *17*, 1326–1342.

Tchekanda, E., Sivanesan, D., & Michnick, S. W. (2014). An infrared reporter to detect spatiotemporal dynamics of protein–protein interactions. *Nature Methods*, *11*, 641–644.

Teuling, E., Haasdijk, E., Demmers, J., Jaarsma, D., Hoogenraad, C. C., Akhmanova, A., Steinmetz, M. O., & Ahmed, S. (2007). Motor neuron disease-associated mutant vesicle-associated membrane protein-associated protein (VAP) B recruits wild-type VAPs into endoplasmic reticulum-derived tubular aggregates. *Journal of Neuroscience*, *27*, 9801–9815.

Tubbs, E., & Rieusset, J. (2016). Study of endoplasmic reticulum and mitochondria interactions by in situ proximity ligation assay in fixed cells. *Journal of Visualized Experiments*, *118*, e54899.

Tubbs, E., Theurey, P., Vial, G., Bendridi, N., Bravard, A., Chauvin, M. A., … Vidal, H. (2014). Mitochondria-associated endoplasmic reticulum membrane (MAM) integrity is required for insulin signaling and is implicated in hepatic insulin resistance. *Diabetes*, *63*, 3279–3294.

Vance, J. E. (1990). Phospholipid synthesis in a membrane fraction associated with mitochondria. *Journal of Biological Chemistry*, *265*, 7248–7256.

Yang, Z., Zhao, X., Xu, J., Shang, W., & Tong, C. (2018). A novel fluorescent reporter detects plastic remodeling of mitochondria–ER contact sites. *Journal of Cell Science*, *131*, jcs208686.

Young, P. A., Senkal, C. E., Suchanek, A. L., Grevengoed, T. J., Lin, D. D., Zhao, L., … Coleman, R. A. (2018). Long-chain acyl-CoA synthetase 1 interacts with key proteins that activate and direct fatty acids into niche hepatic pathways. *Journal of Biological Chemistry*, *293*, 16724–16740.

Zaar, K., Völkl, A., & Fahimi, H. D. (1987). Association of isolated bovine kidney cortex peroxisomes with endoplasmic reticulum. *Biochimica et Biophysica Acta (BBA)-Biomembranes*, *897*, 135–142.

Zhao, Y. G., Liu, N., Miao, G., Chen, Y., Zhao, H., & Zhang, H. (2018). The ER contact proteins VAPA/B interact with multiple autophagy proteins to modulate autophagosome biogenesis. *Current Biology*, *28*, 1234–1245.